NATIONAL AERONAUTICS AND SPACE ADMINISTRATION

Technical Report 32-1582

Parametric Performance Characteristics and Treatment of Temperature Coefficients of Silicon Solar Cells for Space Application

R.E. Patterson
R. K. Yasui

JET PROPULSION LABORATORY
CALIFORNIA INSTITUTE OF TECHNOLOGY
PASADENA, CALIFORNIA

May 15, 1973

NATIONAL AERONAUTICS AND SPACE ADMINISTRATION

Technical Report 32-1582

Parametric Performance Characteristics and Treatment of Temperature Coefficients of Silicon Solar Cells for Space Application

R.E. Patterson
R. K. Yasui

JET PROPULSION LABORATORY
CALIFORNIA INSTITUTE OF TECHNOLOGY
PASADENA, CALIFORNIA

May 15, 1973

Preface

The work described in this Report was performed by the Guidance and Control Division of the Jet Propulsion Laboratory.

Acknowledgment

The authors wish to thank R. F. Greenwood and R. L. Mueller for their careful fabrication of solar cell test plates and accurate solar cell measurements. The assistance given by B. Anspaugh in performance modeling is acknowledged. Also appreciated are the efforts of T. Talbot, who assisted greatly with the development of the computer program interpolation scheme.

Contents

Tables

Contents (contd)

Figures

Abstract

The electrical performance characteristics of 2 and 10 Ω-cm N/P-type silicon solar cells were measured at simulated solar intensities of 5, 50, 100, 140, 250, 400, 550, 700, and 850 mW/cm². At each intensity, the temperature was varied in increments of 20° between extremes of +160 and −160°C. Short-circuit current, open-circuit voltage, and maximum power are presented in graphical format. Also described are three methods for predicting solar cell electrical performance as a function of temperature and intensity. Two of the methods are suitable for use at extreme temperature–intensity conditions. These methods were used successfully to predict the performance of the $I_{sc} - V_{oc}$ transducer on board the Mariner Mars 1971 spacecraft.

Parametric Performance Characteristics and Treatment of Temperature Coefficients of Silicon Solar Cells for Space Application

I. Introduction

Silicon solar cell arrays have proven themselves as the most practical, reliable, and efficient source of electrical power for planetary spacecraft missions flown to date. One of the important prerequisites for successful design and operation of a solar array for a particular mission is the ability to accurately predict its performance characteristics over the appropriate solar intensity and temperature ranges. A major problem that limits prediction accuracy, particularly for missions involving temperature–intensity extremes, is the lack of good experimental test programs to provide statistically significant empirical test data. This lack of test data has limited design tradeoff studies and the development of solar array technology. In addition, methods for predicting solar cell performance for near-Earth missions are not suitable for application to extreme temperature–intensity mission predictions without sacrificing accuracy. As a result, JPL has, over the years, engaged in a comprehensive study of the electrical and mechanical performance behavior of both conventional and nonconventional silicon solar cells for missions over the appropriate range of temperature–intensity conditions from Mercury to Jupiter. Also, JPL has developed several suitable methods for predicting solar cell performance under extreme temperature–intensity conditions. The methods, which are well suited for computer computation, were developed with a minimum use of derived quantities; the identity of the raw parametric data on which they are based was therefore preserved. A condensed version of this report (Ref. 1) was presented at the 7th IECEC held in San Diego, California, on September 25–29, 1972.

II. Experimental Approach

A. Solar Cell Description

The silicon solar cells of 2 and 10 Ω-cm base resistivity discussed in this report were fabricated by Centralab and Heliotek, respectively. In order to maintain a common base line, the cells are similar in all other respects. Both cell types are N/P, are typically 0.046 cm (18 mils) thick, have a surface area of 4 cm^2, have solder-coated titanium–silver vacuum-evaporated bar contacts, and were assembled using a solder reflow technique (Ref. 2). A fused silica coverglass, Cornings glass works 7940, 0.051 cm (20 mils) thick, was bonded to each cell with General Electric RTV-602/SRC05 silicone adhesive.

B. Apparatus

The electrical parametric studies performed consisted of generating current voltage characteristics of two basic types of silicon solar cells over the appropriate range of temperature–intensity, equivalent to that encountered during Mercury and Jupiter missions. Figure 1 shows an overall view of the test facility used throughout the course of these investigations. A multi-cell thermal vacuum test chamber was employed in conjunction with a solar simulator, which approximates the intensity and spectrum of space sunlight.

A Spectrolab Model X25 Mark II, close-filtered, dry nitrogen-purged solar simulator was used throughout the test program. In order to achieve the broad range of solar intensities required, two separate lenticular optical units were used, one for solar intensities from 250 to 5 mW/cm^2 and the other for intensities from 250 to 850 mW/cm^2. Intermediate intensities were obtained by interposing various types of screens within the light path and adjusting the current to the xenon source. Balloon flight standard cells comprising an intensity reference cell and two separate cells having narrow-bandpass filters were mounted within the test chamber. The latter cells were used to determine

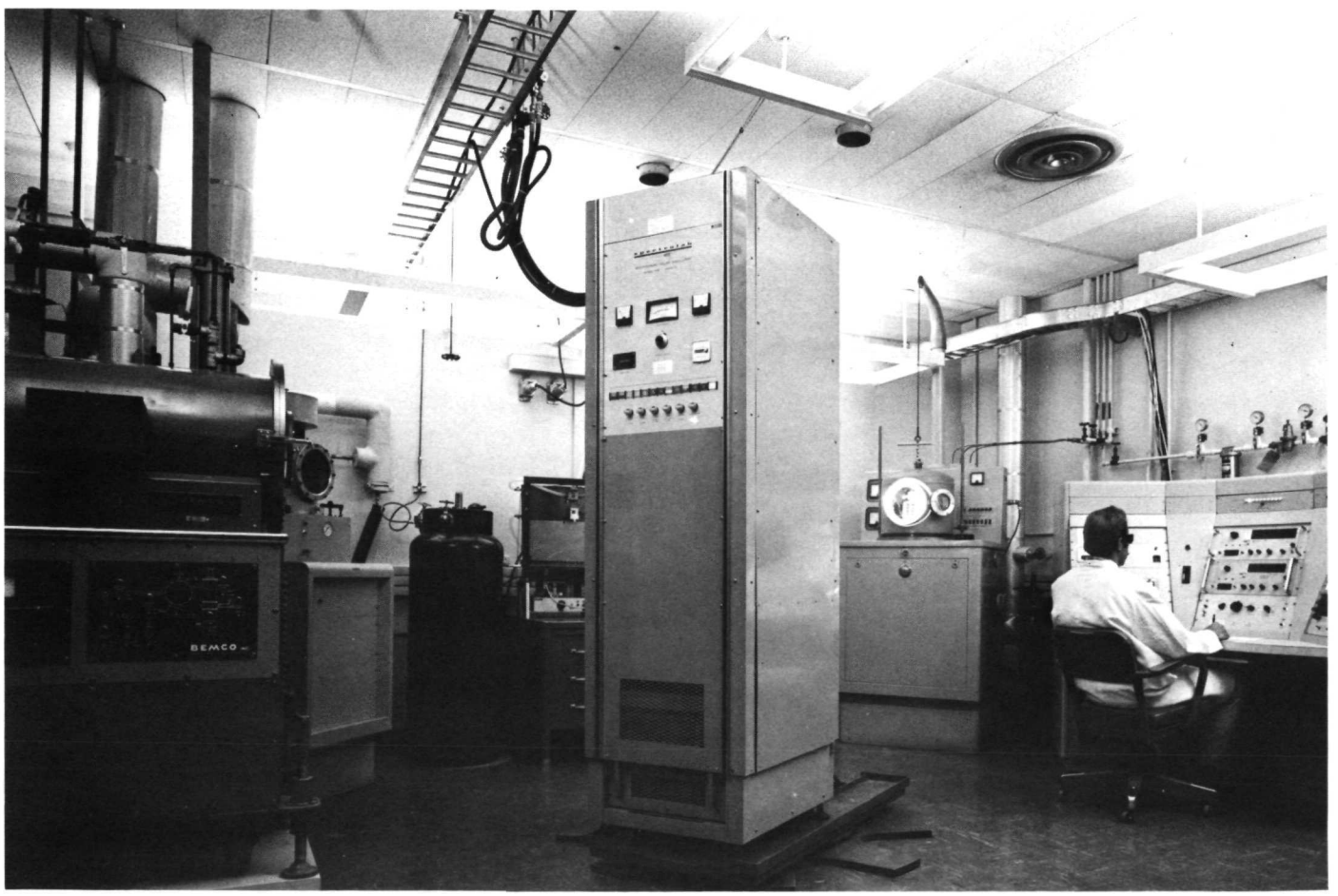

Fig. 1. Solar energy developmental and test facility

the spectral quality of the solar simulator by observing its red-to-blue ratio during test.

Electrical connection to each cell was made with four wires in order to prevent voltage drop across the current-carrying pair from influencing the voltage readings. A typical solar cell parametric test plate composed of filtered cells, thermocouples, interconnectors, printed circuit board, and wiring harness is shown in Fig. 2 as viewed through the quartz window of the test chamber. The solar cells are bonded to a 0.318-cm (0.125-in.) thick copper plate using General Electric RTV-560 silicone adhesive and primer. The electrical characteristics of each cell tested are obtained in the form of a current–voltage curve using a Hewlett Packard Model 7030 XY recorder. The short-circuit current and open-circuit voltage parameters are obtained on a five-place readout, integrating-type digital voltmeter. The operating temperature of the solar cells was controlled within ± 0.5°C using copper–constantan thermocouples and a proportional temperature controller. Because of the extreme temperature range covered in this study (-160 to $+160$°C), solar cells were soldered to tinned Kovar interconnectors. (Kovar is a metal alloy which approaches the thermal expansion coefficient of silicon.) The cell temperature was varied in increments of 20° between temperature extremes of $+160$ and -160°C.

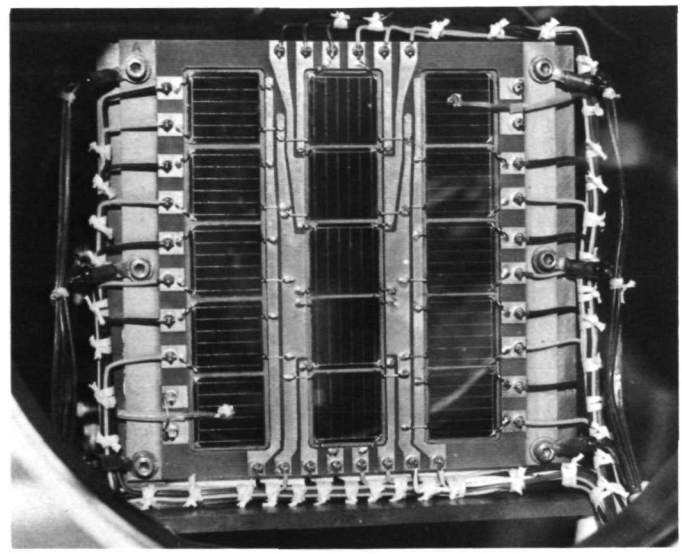

Fig. 2. Test specimens and standard cells as viewed through the quartz window of the test chamber

III. Graphical Presentation of Parametric Data

All data presented in this report are based on the average of 15 cells in each of two groups, one from Heliotek and the second from Centralab. Figure 3 shows the results of plotting short-circuit current (I_{sc}) vs. solar intensity, with temperature as a parameter, for both 2 and 10 Ω-cm cells. The 2 Ω-cm cell I_{sc} is linear with intensity over the temperature–intensity range studied. However, the 10 Ω-cm cell I_{sc} does not behave linearly above 250 mW/cm² and 100°C. The nonlinear behavior of the 10 Ω-cm cells is probably due to the higher series resistance of these cells. The linear behavior of the 2 Ω-cm cell makes it a much better candidate for a standard cell used in adjusting and monitoring solar simulator intensity. Also shown in Fig. 3 is the I_{sc} dependence on temperature. At least three separate factors contribute to reduced I_{sc} at lower temperature. As temperature decreases, the band gap increases and fewer incident photons can generate current. Dash and Newman (Ref. 3) have shown that light absorption (necessary for the generation of current) decreases with temperature from 27 to -196°C. Also, reduced collection of current carriers as temperature decreases results from a decrease in diffusion lengths at lower temperature.

Figure 4 shows the results of plotting open-circuit voltage V_{oc} vs. the $\log_{10}$ of solar intensity, with temperature as a parameter, for both 2 and 10 Ω-cm cells. The V_{oc} of both cell types is a logarithmic function of intensity over the range of 25 to 850 mW/cm².

Maximum power P_{mp} of both 2 and 10 Ω-cm cell types is plotted vs. solar intensity, with temperature as a parameter, in Fig. 5. As expected, P_{mp} increases with intensity, since both I_{sc} and V_{oc} increase with intensity. However, at higher intensities (> 250 mW/cm²), P_{mp} of the 10 Ω-cm cells falls off with respect to P_{mp} of the 2 Ω-cm cells. Thus the 10 Ω-cm cells would not be good candidates for near-Sun missions. Also seen in Fig. 5 is the increase in P_{mp} with decreased temperature. Thus, the rate of increase in V_{oc} with decreased temperature is dominant over the rate of decrease of other parameters such as I_{sc}. The spread in maximum power, as reflected by standard deviations, is seen to be greater at the low and high intensity extremes. This is as expected, since the cells used in this study were selected such that their maximum powers were matched at 1 AU equivalent solar intensity and 28°C temperature. The variability exhibited in P_{mp} would cause serious mismatch problems in an array, which would result in a decrease in operating efficiency. As planetary exploration missions are extended toward inner and outer planets, further attention must be focused on cell fabrication processes, proper selection of materials, and cell screening techniques in order to ensure optimum performance.

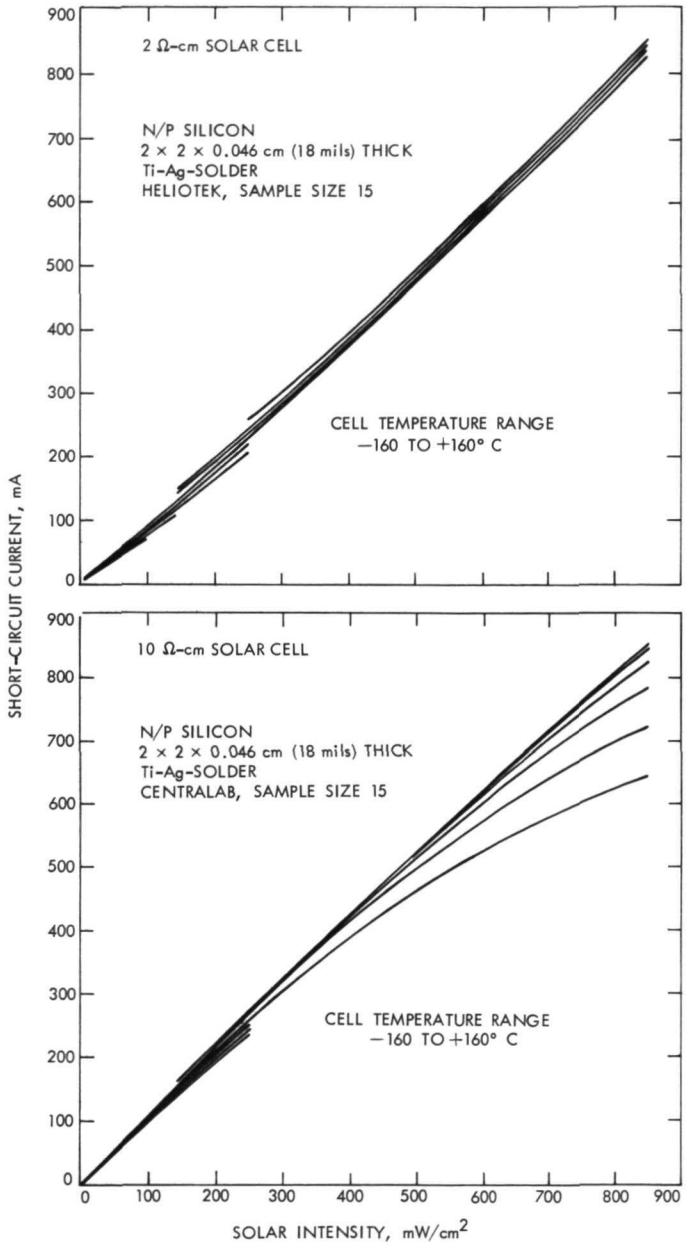

Fig. 3. Short-circuit current output as a function of intensity and cell temperature

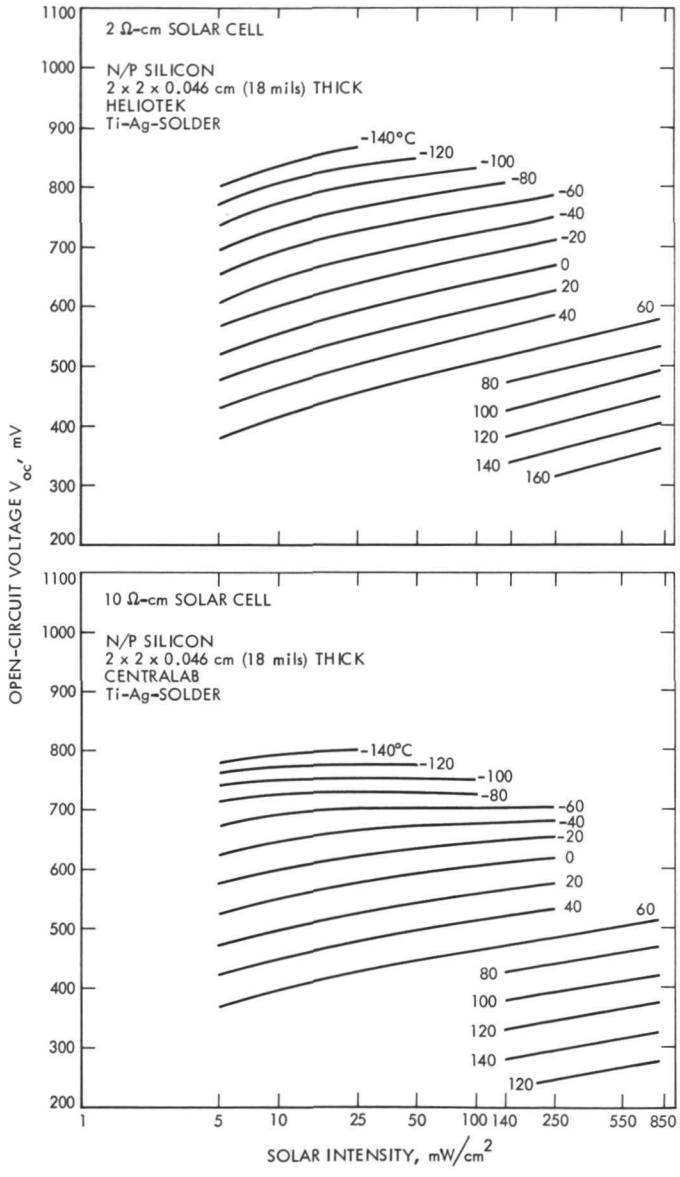

Fig. 4. Open-circuit voltage output as a function of intensity and cell temperature

IV. Solar Cell Modeling for Performance Predictions

The parametric presentation of the solar cell electrical performance data in Figs. 3 through 5 is useful in terms of describing both a quantitative and qualitative relationship between solar cell output and temperature–intensity conditions. However, the quantitative description is limited in resolution in accordance with the number of temperature–intensity test conditions examined. Thus, in order to predict the performance characteristics of silicon solar cells over a continuous range of temperature–intensity conditions, it is necessary to model the electrical performance of the solar cells. Three methods for modeling the parametric data in order to predict solar cell performance are discussed below, together with the characteristic advantages and disadvantages of each. In general, the selection of one method over another involves trading off accuracy with complexity.

A. Method 1: Analytical Expression 1

This method has been previously described by Sandstrom (Ref. 4). The following equations are used to translate short-circuit current and open-circuit voltage from a reference temperature–intensity T_0, H_0 to a new temperature–intensity T_i, H_i:

$$I_{sc}(T_i, H_i) = I_{sc}(H_0, T_0)\frac{H_i}{H_0} + \alpha_{H_i}(T_i - T_0) \qquad (1)$$

$$V_{oc}(T_i, H_i) = V_{oc}(H_0, T_0) - \beta_{H_i}(T_i - T_0) - \Delta I_{sc}R_s \qquad (2)$$

$$\Delta I_{sc} = I_{sc}(T_i, H_i) - I_{sc}(T_0, H_0) \qquad (3)$$

The series resistance R_s is treated as a constant. The short-circuit current temperature coefficient α and the open-circuit voltage temperature coefficient β are defined as the magnitude of the slope of the curves which express I_{sc} and V_{oc}, respectively, as a function of temperature at a given intensity. That is,

$$\alpha_{H_i} = \frac{dI_{sc}}{dT} \qquad (4)$$

and

$$\beta_{H_i} = \frac{dV_{oc}}{dT} \qquad (5)$$

at constant intensity H_i.

Although this method is easy to apply, it suffers several shortcomings. The coefficients α and β do vary with temperature, and thus the valid application of Eqs. (1) and (2) is limited to a relatively small temperature range. Also, Eq. (2) does not explicitly reveal the logarithmic dependence of V_{oc} on intensity which was shown in Fig. 4.

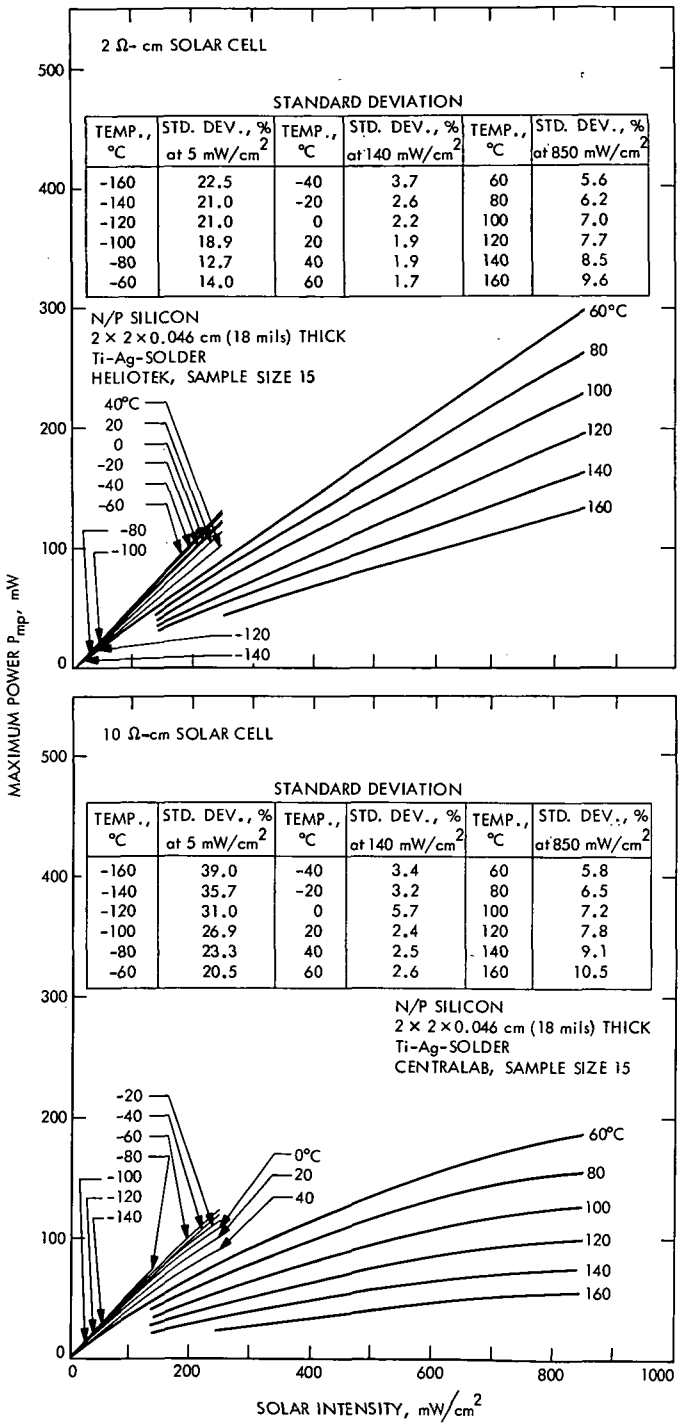

Fig. 5. Maximum power output as a function of intensity and cell temperature

Table 1. Average short-circuit currents and standard deviations for 2 Ω-cm cells

Temperature, °C	Solar intensity,[a] mW/cm²									
	5.00	25.00	50.00	100.00	140.00	250.00	400.00	550.00	700.00	850.00
−160	3.62 (0.28)	–	–	–	–	–	–	–	–	–
−140	3.67 (0.27)	17.72 (1.05)	–	–	–	–	–	–	–	–
−120	3.53 (0.28)	17.87 (0.95)	36.69 (2.06)	–	–	–	–	–	–	–
−100	3.62 (0.27)	18.29 (0.89)	37.63 (1.90)	73.79 (3.08)	–	–	–	–	–	–
−80	3.77 (0.27)	19.18 (0.73)	38.75 (1.48)	77.18 (2.66)	109.62 (4.41)	–	–	–	–	–
−60	3.95 (0.26)	19.81 (0.60)	40.48 (1.20)	81.93 (1.96)	116.12 (3.07)	209.25 (6.41)	–	–	–	–
−40	4.13 (0.26)	20.79 (0.46)	42.16 (1.03)	85.51 (1.53)	121.98 (2.68)	221.10 (5.46)	–	–	–	–
−20	4.33 (0.26)	21.25 (0.73)	43.16 (0.87)	88.30 (1.74)	126.05 (2.33)	228.45 (5.24)	–	–	–	–
0	4.41 (0.22)	22.39 (0.35)	43.91 (0.77)	91.96 (1.33)	129.33 (2.28)	234.35 (5.38)	–	–	–	–
20	4.46 (0.27)	23.23 (0.34)	45.39 (0.93)	93.45 (1.02)	133.09 (2.10)	239.20 (5.14)	–	–	–	–
40	4.86 (0.17)	23.55 (0.34)	46.51 (0.84)	94.83 (1.15)	134.85 (1.96)	239.11 (4.81)	–	–	–	–
60	4.90 (0.16)	23.83 (0.34)	47.17 (0.74)	95.77 (1.27)	134.16 (1.82)	242.15 (4.70)	374.42 (9.93)	514.25 (14.81)	672.31 (11.14)	835.33 (13.24)
80	–	–	–	–	136.29 (1.96)	245.89 (4.53)	377.79 (9.15)	521.71 (11.67)	672.77 (10.16)	842.89 (12.22)
100	–	–	–	–	136.02 (1.98)	249.07 (4.57)	378.44 (10.51)	525.64 (11.30)	676.17 (9.50)	850.05 (12.27)
120	–	–	–	–	137.28 (1.96)	249.62 (4.43)	387.15 (10.17)	526.78 (8.41)	683.42 (9.70)	856.10 (11.94)
140	–	–	–	–	139.13 (2.03)	252.56 (4.59)	395.12 (10.14)	537.79 (11.80)	679.29 (10.37)	857.11 (13.94)
160	–	–	–	–	–	255.21 (4.29)	398.19 (10.06)	532.66 (8.22)	685.62 (12.54)	860.11 (19.39)

[a]Standard deviations are given in parentheses.

Equations (1) and (2) have been used to successfully predict solar cell performance for near-Earth conditions; however, because of the limitations discussed above, methods 2 and 3 were developed.

B. Method 2: Analytical Expression 2

This method was developed for the purpose of providing an analytical expression well suited for computer computation which could be used for predicting I_{sc} and V_{oc} over a wide range of both temperature and intensity. Also, it was desired to take into account the relative uncertainty of the parametric data. The I_{sc} and V_{oc} parametric data (average output of 15 cells with standard deviations) of the 2 and 10 Ω-cm cells are tabulated in Tables 1 through 4.

The V_{oc} and the I_{sc} models were developed in a similar manner. The development of the V_{oc} model will be discussed in detail. To avoid repetition, only the final results of the I_{sc} model will be described.

1. Development of V_{oc} Model. The first step was to obtain an expression which described V_{oc} performance as a function of intensity at constant temperature T_i. The following equation was found to fit both the 2 and 10 Ω-cm parametric data quite well over the intensity range of 25 to 850 mW/cm²:

$$V_{oc}(T_i, H) = A_{T_i} + B_{T_i} \log_{10} H \qquad (6)$$

Table 2. Average short-circuit currents and standard deviations for 10 Ω-cm cells

Temperature, °C	Solar intensity,[a] mW/cm²									
	5.00	25.00	50.00	100.00	140.00	250.00	400.00	550.00	700.00	850.00
−160	4.38 (0.22)	–	–	–	–	–	–	–	–	–
−140	4.48 (0.19)	21.49 (0.63)	–	–	–	–	–	–	–	–
−120	4.62 (0.16)	22.04 (0.44)	44.30 (0.63)	–	–	–	–	–	–	–
−100	4.73 (0.14)	22.52 (0.34)	45.30 (0.46)	91.05 (1.42)	–	–	–	–	–	–
−80	4.79 (0.13)	22.88 (0.34)	45.99 (0.36)	93.01 (1.35)	130.65 (2.49)	–	–	–	–	–
−60	4.87 (0.14)	23.52 (0.34)	46.29 (0.31)	95.81 (1.00)	132.65 (2.50)	237.40 (1.78)	–	–	–	–
−40	4.73 (0.11)	23.90 (0.34)	47.33 (0.30)	96.92 (0.95)	135.39 (3.29)	240.88 (1.95)	–	–	–	–
−20	4.73 (0.12)	24.36 (0.36)	48.50 (0.27)	98.83 (0.99)	137.41 (2.96)	245.55 (2.14)	–	–	–	–
0	4.81 (0.13)	24.79 (0.32)	48.79 (0.33)	100.55 (1.21)	141.05 (2.91)	252.99 (2.15)	–	–	–	–
20	4.79 (0.13)	25.26 (0.34)	50.43 (0.38)	102.64 (1.13)	145.57 (3.16)	258.54 (1.82)	–	–	–	–
40	4.89 (0.14)	25.64 (0.36)	51.46 (0.41)	104.05 (1.12)	145.39 (3.20)	261.90 (2.08)	–	–	–	–
60	4.98 (0.13)	25.92 (0.36)	52.25 (0.39)	105.31 (1.15)	147.02 (3.26)	265.02 (2.13)	412.71 (4.03)	575.35 (6.31)	717.70 (9.17)	850.13 (13.95)
80	–	–	–	–	148.34 (3.57)	267.92 (2.22)	415.52 (4.17)	577.60 (8.04)	717.05 (9.63)	840.63 (19.48)
100	–	–	–	–	149.85 (3.50)	265.04 (1.96)	416.19 (4.48)	576.09 (8.20)	708.15 (11.87)	820.55 (27.22)
120	–	–	–	–	154.22 (3.53)	266.89 (3.30)	415.55 (5.04)	567.68 (11.13)	686.22 (17.59)	779.98 (33.46)
140	–	–	–	–	154.95 (3.46)	274.97 (2.15)	411.10 (7.02)	538.27 (15.03)	642.26 (24.80)	723.32 (39.31)
160	–	–	–	–	–	257.56 (4.98)	387.45 (11.49)	496.61 (21.22)	580.27 (30.41)	646.08 (39.31)

[a]Standard deviations are given in parentheses.

The coefficients A_{T_i} and B_{T_i} were found for each temperature by a least-squares fit to the parametric data, weighted according to the inverse standard deviation σ of each data point. That is, at temperature T_i, A_{T_i} and B_{T_i} were found such as to minimize the following summation:

$$\sum_j \left\{ \frac{V_{oc}(T_i, H_j) - (A_{T_i} + B_{T_i} \log H_j)}{\sigma(T_i, H_j)} \right\}^2 \quad (7)$$

No attempt was made to counterweight the least-squares fit to "neutralize" the weighting incurred by taking the log of intensity.

The temperature dependence of the A_{T_i} and the B_{T_i} was found empirically. Polynomials of first through fifth order were fitted individually to both the A_{T_i} and B_{T_i} vs. temperature plots. Fifth-order polynomials gave the best fit for both $A(T)$ and $B(T)$. Thus, $A(T)$ and $B(T)$ take the following form:

$$A(T) = a_0 + a_1T + a_2T^2 + a_3T^3 + a_4T^4 + a_5T^5 \quad (8)$$

$$B(T) = b_0 + b_1T + b_2T^2 + b_3T^3 + b_4T^4 + b_5T^5 \quad (9)$$

Table 3. Average open-circuit voltages and standard deviations for 2 Ω-cm cells

Temperature, °C	Solar intensity,[a] mW/cm²									
	5.00	25.00	50.00	100.00	140.00	250.00	400.00	550.00	700.00	850.00
−160	834.48									
	(46.90)	–	–	–	–	–	–	–	–	–
−140	801.05	866.62								
	(39.67)	(23.51)	–	–	–	–	–	–	–	–
−120	772.26	837.71	849.79							
	(32.50)	(13.47)	(15.58)	–	–	–	–	–	–	–
−100	735.09	805.89	824.37	830.75						
	(23.07)	(7.01)	(8.40)	(10.42)	–	–	–	–	–	–
−80	693.93	765.08	785.50	800.18	808.45					
	(18.11)	(5.00)	(5.30)	(5.05)	(5.99)	–	–	–	–	–
−60	653.18	725.24	746.55	765.28	771.85	786.66				
	(14.75)	(3.98)	(3.31)	(4.07)	(4.51)	(6.75)	–	–	–	–
−40	608.94	681.66	705.83	724.30	737.19	752.17				
	(13.00)	(3.11)	(2.53)	(3.00)	(3.68)	(6.10)	–	–	–	–
−20	565.54	537.40	661.98	682.20	696.16	713.61				
	(10.81)	(2.65)	(2.11)	(2.28)	(2.72)	(4.32)	–	–	–	–
0	519.85	591.68	617.92	640.62	653.12	671.95				
	(9.73)	(2.53)	(1.63)	(2.03)	(2.19)	(3.22)	–	–	–	–
20	473.01	547.15	572.38	596.75	609.85	629.41				
	(9.38)	(2.54)	(1.89)	(1.85)	(1.93)	(2.65)	–	–	–	–
40	427.12	500.85	526.35	549.89	564.43	585.13				
	(7.87)	(2.55)	(1.83)	(1.96)	(2.26)	(2.66)	–	–	–	–
60	378.13	453.61	480.29	504.73	518.80	541.20	553.63	564.43	572.46	580.38
	(7.27)	(2.89)	(2.20)	(2.27)	(2.35)	(2.67)	(2.83)	(3.32)	(4.35)	(5.31)
80					471.67	495.48	509.54	519.92	529.52	537.30
	–	–	–	–	(2.62)	(2.71)	(3.24)	(3.94)	(3.93)	(4.91)
100					425.38	449.48	466.34	477.19	486.61	493.28
	–	–	–	–	(2.74)	(2.92)	(3.16)	(3.18)	(4.60)	(5.36)
120					379.29	403.94	422.49	432.59	442.65	450.24
	–	–	–	–	(2.80)	(2.95)	(3.33)	(3.51)	(4.28)	(5.06)
140					333.72	357.35	378.30	389.32	398.93	406.40
	–	–	–	–	(2.78)	(3.52)	(2.97)	(3.48)	(4.29)	(5.29)
160						312.08	333.28	344.88	354.88	362.48
	–	–	–	–	–	(2.99)	(2.92)	(3.69)	(4.52)	(5.47)

[a]Standard deviations are given in parentheses.

Table 4. Average open-circuit voltages and standard deviations for 10 Ω-cm cells

Temperature, °C	Solar intensity,[a] mW/cm²									
	5.00	25.00	50.00	100.00	140.00	250.00	400.00	550.00	700.00	850.00
−160	748.38 (95.76)	–	–	–	–	–	–	–	–	–
−140	775.15 (74.95)	799.57 (21.75)	–	–	–	–	–	–	–	–
−120	761.75 (50.28)	774.55 (20.43)	771.32 (21.03)	–	–	–	–	–	–	–
−100	742.28 (30.28)	752.01 (20.86)	751.59 (21.84)	748.30 (23.71)	–	–	–	–	–	–
−80	712.06 (18.27)	729.50 (19.96)	730.38 (22.26)	727.95 (24.26)	726.61 (23.24)	703.65 (24.64)	–	–	–	–
−60	671.44 (12.73)	701.81 (16.19)	706.35 (20.01)	707.47 (22.52)	707.06 (23.47)	682.18 (23.39)	–	–	–	–
−40	622.32 (10.86)	664.17 (10.41)	674.55 (15.09)	681.40 (19.27)	681.55 (20.88)	652.53 (19.19)	–	–	–	–
−20	573.46 (9.47)	620.71 (5.60)	634.25 (9.30)	646.38 (13.92)	649.84 (15.97)	617.85 (14.00)	–	–	–	–
0	522.92 (8.47)	572.76 (3.12)	590.65 (5.15)	605.38 (8.61)	610.96 (10.51)	577.44 (9.29)	–	–	–	–
20	470.94 (7.45)	524.32 (2.75)	544.13 (3.39)	560.22 (5.24)	568.31 (6.45)	533.95 (6.28)	–	–	–	–
40	419.75 (6.80)	475.60 (2.99)	495.21 (3.14)	512.84 (3.72)	522.12 (4.65)	488.53 (4.97)	497.22 (5.77)	505.55 (6.87)	510.02 (7.30)	512.75 (7.47)
60	367.48 (5.97)	425.50 (3.18)	446.62 (3.45)	466.42 (3.74)	475.02 (3.95)	440.91 (4.78)	451.02 (5.25)	459.19 (6.15)	464.02 (6.39)	467.15 (7.30)
80	–	–	–	–	427.74 (4.34)	390.99 (4.88)	403.42 (5.33)	412.34 (6.16)	417.72 (6.18)	420.22 (6.99)
100	–	–	–	–	379.47 (4.38)	341.22 (4.98)	355.19 (5.38)	364.48 (6.02)	369.31 (6.66)	372.91 (7.02)
120	–	–	–	–	330.45 (4.82)	294.65 (5.03)	308.23 (5.69)	314.97 (6.03)	321.32 (6.68)	324.88 (7.03)
140	–	–	–	–	280.46 (5.11)	244.52 (5.31)	257.80 (5.91)	266.90 (6.15)	272.53 (6.55)	277.72 (8.76)
160	–	–	–	–	–	–	–	–	–	–

[a]Standard deviations are given in parentheses.

The a_i and b_i are presented in Table 5. The complete expression for $V_{oc}(T, H)$ is

$$V_{oc}(T,H) = A(T) + B(T)\log_{10} H$$
$$= a_0 + a_1T + a_2T^2 + a_3T^3 + a_4T^4 + a_5T^5$$
$$+ (b_0 + b_1T + b_2T^2 + b_3T^3 + b_4T^4$$
$$+ b_5T^5)\log_{10} H \qquad (10)$$

Although the expression for $V_{oc}(T, H)$ has many terms, it is well suited for computer computation. Thus, the entire array of parametric data for each cell type can be characterized by Eq. (10), together with the appropriate values for the 12 coefficients. Equation (10) was evaluated for both the 2 and 10 Ω-cm cells at each of the temperature–intensity conditions under which experimental data were taken. The percent difference between the computed V_{oc} (using Eq. 10) and the actual V_{oc} was calculated for each of the temperature–intensity conditions according to the expression

$$\text{percent difference}\,(T_i, H_i) = 100\,\frac{\text{calculated } V_{oc}(T_i,H_i) - \text{actual } V_{oc}(T_i,H_i)}{1/2\,\text{calculated } V_{oc}(T_i,H_i) + \text{actual } V_{oc}(T_i,H_i)} \qquad (11)$$

The percent differences are tabulated for both 2 and 10 Ω-cm cells in Tables 6 and 7.

It was found that, in general, the computed V_{oc} agree quite well with the actual ones, the maximum difference occurring at 5 mW/cm² (1 to 6%). However, from 25 to 850 mW/cm², all of the percent differences are less than 1% for 2 Ω-cm cells, whereas all but four of the percent differences are less than 1% for the 10 Ω-cm cells. Although Eq. (10) does not explicitly contain a temperature coefficient term, a point value of β can be determined at any temperature T_0 and intensity H_0 by differentiating Eq. (10) with respect to the temperature holding intensity constant and then evaluating the derivative at (T_0, H_0).

Also, Eq. (10) can be used to evaluate the average temperature coefficient $\bar{\beta}(T, H)$ over a temperature range T_j to T_k at some intensity H_i. The appropriate expression is

$$\text{average temperature coefficient} = \bar{\beta}(T_j \text{ to } T_k, H_i)$$
$$= \frac{a_1(T_k - T_j) + a_2(T_k^2 - T_j^2) + a_3(T_k^3 - T_j^3) + a_4(T_k^4 - T_j^4) + a_5(T_k^5 - T_j^5)}{T_k - T_j}$$
$$+ \frac{[+b_1(T_k - T_j) + b_2(T_k^2 - T_j^2) + b_3(T_k^3 - T_j^3) + b_4(T_k^4 - T_j^4) + b_5(T_k^5 - T_j^5)]\log_{10} H_i}{T_i - T_j} \qquad (12)$$

Again, this expression is well suited for computer computation.

2. Development of I_{sc} Model. The following expression was found to describe the I_{sc} performance as a function of intensity at constant temperature T_i:

$$I_{sc}(T_i, H) = C_{T_i}H \qquad (13)$$

Equation (13) fits the 2 Ω-cm data quite well over the entire range of intensities (5 to 850 mW/cm²), whereas the fit for the 10 Ω-cm data was good only from 5 to 250 mW/cm². However, since 10 Ω-cm cells are not likely to be used for near-Sun missions, as discussed previously, they were not modeled for intensities greater than 250 mW/cm².

The temperature dependence of $C(T)$ was found by the same method used for $A(T)$ and $B(T)$. The complete expression for I_{sc} takes the form

$$I_{sc}(T,H) = (c_0 + c_1T + c_2T^2 + c_3T^3 + c_4T^4 + c_5T^5)H \qquad (14)$$

Although Eq. (14) does not explicitly contain a temperature coefficient term, a point value of α can be determined at any temperature T_0 and intensity H_0 by differentiating Eq. (14) with respect to the temperature holding intensity constant and then evaluating the derivative at (T_0, H_0). Also, Eq. (14) can be used to determine the average short-circuit temperature coefficient $\bar{\alpha}(T_k - T_j, H_i)$ over a temperature range T_j to T_k at intensity H_i. The expression is

$$\bar{\alpha}(T_k - T_j, H_i) = [c_1(T_k - T_j) + c_2(T_k^2 - T_j^2)$$
$$+ c_3(T_k^3 - T_j^3) + c_4(T_k^4 - T_j^4)$$
$$+ c_5(T_k^5 - T_j^5)]\frac{H_i}{T_k - T_j} \qquad (15)$$

Equation (14) was used to calculate I_{sc} at each of the temperature–intensity conditions at which experimental data were taken, as shown in Tables 1 and 2. The percent differences between the calculated and actual I_{sc} for both the 2 and 10 Ω-cm cells were evaluated and are presented in Tables 8 and 9. It was found that most of the differences fall in the range of 0 to 3% for both types of cells.

Table 5. Coefficients for analytical expression[a,b]

V_{oc} expression $V_{oc} = A(T) + B(T) \log_{10} H$ $A(T) = a_0 + a_1T^1 + a_2T^2 + a_3T^3 + a_4T^4 + a_5T^5$ $B(T) = b_0 + b_1T^1 + b_2T^2 + b_3T^3 + b_4T^4 + b_5T^5$		I_{sc} expression $I_{sc} = C(T)\,H$ $C(T) = c_0 + c_1T^1 + c_2T^2 + c_3T^3 + c_4T^4 + c_5T^5$
2 Ω-cm cells[c]		
$a_0 =$ 0.480653 + 03	$b_0 =$ 0.801129 + 02	$c_0 =$ 0.914727 + 00
$a_1 =$ −0.241702 + 01	$b_1 =$ 0.118309 + 00	$c_1 =$ 0.108713 − 02
$a_2 =$ 0.294965 − 02	$b_2 =$ −0.224011 − 02	$c_2 =$ −0.695706 − 05
$a_3 =$ −0.206159 − 04	$b_3 =$ 0.140478 − 04	$c_3 =$ 0.226603 − 07
$a_4 =$ −0.184560 − 06	$b_4 =$ 0.816163 − 07	$c_4 =$ 0.171090 − 09
$a_5 =$ 0.114636 − 08	$b_5 =$ −0.548025 − 09	$c_5 =$ −0.144039 − 11
10 Ω-cm cells[d]		
$a_0 =$ 0.507642 + 03	$b_0 =$ 0.480243 + 02	$c_0 =$ 0.100584 + 01
$a_1 =$ −0.300212 + 01	$b_1 =$ 0.455891 + 00	$c_1 =$ 0.143787 − 02
$a_2 =$ 0.407518 − 02	$b_2 =$ −0.470785 − 02	$c_2 =$ −0.315471 − 05
$a_3 =$ 0.459916 − 04	$b_3 =$ −0.909273 − 05	$c_3 =$ −0.121720 − 06
$a_4 =$ −0.323551 − 06	$b_4 =$ 0.205860 − 06	$c_4 =$ 0.538927 − 10
$a_5 =$ −0.164756 − 09	$b_5 =$ −0.323078 − 09	$c_5 =$ 0.462234 − 11

[a]Coefficients are in "E" format. The two digits on the right, including the sign, are powers of 10 which multiply the six digits to the left of the powers.

[b]Units: V_{oc} in mV, I_{sc} in mA, H in mW/cm², T in °C.

[c]See Table 6 for applicable temperature intensity range for V_{oc}, Table 8 for I_{sc}.

[d]See Table 7 for applicable temperature intensity range for V_{oc}, Table 9 for I_{sc}.

By comparing Tables 6 and 7 with Tables 8 and 9, it can be seen that the analytical expressions fit the V_{oc} data better than the I_{sc} data. This is to be expected, since temperature is more accurately controlled than intensity during the parametric cell testing; I_{sc} depends linearly on intensity, while V_{oc} is a logarithmic function of intensity. For example, at 140 mW/cm², a ±3% error in intensity causes a corresponding error in I_{sc}, while the effect would be much less than 1% on V_{oc}.

Method 2 was used together with prelaunch trajectory and temperature predictions to predict the Mariner 9 $I_{sc} - V_{oc}$ transducer performance as a function of heliocentric distance. Data from the $I_{sc} - V_{oc}$ transducer during spacecraft flight, together with accurate transducer predictions, have proven to be of significant value in providing engineering information on solar array performance characteristics.

C. Method 3: Computer Program Interpolation Scheme

This method was developed in order to provide a technique for predicting the solar electrical performance over a wide range of temperature–intensity conditions and to

(1) Preserve the original identity of the parametric data by minimizing the use of derived quantities.

(2) Utilize only those parametric data which cover the range of the predictions being made. For example, for a Mercury mission, only the parametric data in the intensity range of 140 to 850 mW/cm² would be used.

(3) Provide a method for propagating parametric data uncertainty (as reflected by standard deviations) through prediction calculations and give some estimate of the uncertainty of the prediction.

This method uses a computer program interpolation scheme. The A_{T_i} and B_{T_i} are found for the V_{oc} data and C_{T_i} are found for the I_{sc} data in exactly the same fashion used in method 2. However, only the parametric data which cover the range of the predictions being made are utilized. Once the A_{T_i}, B_{T_i}, and C_{T_i} are determined at each parametric temperature, Eqs. (6) and (13) are evaluated for each set of A, B, and C (one set per parametric temperature) at the prediction intensity. This method differs from method 2 in that no attempt is made to find the coefficient's functional dependence on temperature. The temperature dependence of V_{oc} and I_{sc} at the prediction intensity is found directly by a "French Curve Fit" (segmented cubic polynomials) of the results obtained by evaluating Eqs. (6) and (13), respectively, at each of the parametric temperatures. The French Curve is then evaluated at the prediction temperature.

Table 6. Comparison of computed and actual V_{oc}, 2 Ω-cm cells (% difference)

Temperature, °C	Solar intensity, mW/cm²									
	5.00	25.00	50.00	100.00	140.00	250.00	400.00	550.00	700.00	850.00
−160	−1.00	–	–	–	–	–	–	–	–	–
−140	3.57	−0.83	–	–	–	–	–	–	–	–
−120	4.76	0.02	0.01	–	–	–	–	–	–	–
−100	5.20	0.03	−0.55	0.33	–	–	–	–	–	–
−80	5.07	0.38	−0.15	0.06	0.02	–	–	–	–	–
−60	4.28	0.12	−0.18	−0.13	0.22	0.36	–	–	–	–
−40	3.80	0.09	−0.30	0.11	−0.23	0.17	–	–	–	–
−20	3.19	0.03	−0.19	0.24	−0.16	0.10	–	–	–	–
0	3.18	0.16	−0.19	0.04	−0.08	0.12	–	–	–	–
20	3.61	0.07	−0.05	−0.01	−0.20	−0.03	–	–	–	–
40	4.00	0.25	0.10	0.32	−0.13	−0.12	–	–	–	–
60	5.17	0.54	0.15	0.24	−0.15	−0.43	0.39	0.50	0.60	0.43
80	–	–	–	–	0.08	−0.46	0.16	0.39	0.23	0.10
100	–	–	–	–	0.14	−0.39	−0.22	0.01	−0.07	0.06
120	–	–	–	–	0.20	−0.33	−0.38	0.16	0.01	−0.00
140	–	–	–	–	0.17	0.11	−0.41	0.09	0.12	0.22
160	–	–	–	–	–	0.19	−0.35	0.12	0.11	0.23

Table 7. Comparison of computed and actual V_{oc}, 10 Ω-cm cells (% difference)

Temperature, °C	Solar intensity, mW/cm²									
	5.00	25.00	50.00	100.00	140.00	250.00	400.00	550.00	700.00	850.00
−160	0.42	–	–	–	–	–	–	–	–	–
−140	0.04	−1.86	–	–	–	–	–	–	–	–
−120	2.17	−0.22	−0.11	–	–	–	–	–	–	–
−100	2.85	0.46	0.05	0.02	–	–	–	–	–	–
−80	3.11	0.27	−0.04	0.11	0.21	–	–	–	–	–
−60	3.37	−0.19	−0.47	−0.26	−0.02	0.77	–	–	–	–
−40	3.86	−0.15	−0.64	−0.61	−0.12	0.65	–	–	–	–
−20	3.66	0.01	−0.36	−0.50	−0.19	0.82	–	–	–	–
0	3.44	0.35	−0.24	−0.28	−0.04	0.80	–	–	–	–
20	3.59	0.46	−0.14	−0.04	−0.05	0.78	–	–	–	–
40	4.06	0.53	0.12	0.12	−0.02	0.53	–	–	–	–
60	5.68	1.08	0.27	−0.18	−0.18	0.09	0.76	0.71	1.03	1.46
80	–	–	–	–	−0.45	−0.16	0.18	0.12	0.36	0.72
100	–	–	–	–	−0.45	0.15	−0.16	−0.49	−0.39	0.11
120	–	–	–	–	−0.14	0.68	−0.18	−0.69	−0.46	−0.20
140	–	–	–	–	0.25	0.24	−0.45	−0.11	−0.25	0.12
160	–	–	–	–	–	0.09	0.02	−0.07	0.34	0.41

Table 8. Comparison of computed and actual I_{sc}, 2 Ω-cm cells (% difference)

Temperature, °C	Solar intensity, mW/cm²									
	5.00	25.00	50.00	100.00	140.00	250.00	400.00	550.00	700.00	850.00
−160	1.24	–	–	–	–	–	–	–	–	–
−140	−3.72	−0.23	–	–	–	–	–	–	–	–
−120	1.44	0.20	−2.42	–	–	–	–	–	–	–
−100	2.90	1.85	−0.98	−1.00	–	–	–	–	–	–
−80	3.82	2.08	1.07	1.49	0.05	–	–	–	–	–
−60	4.08	3.78	1.63	0.44	−0.79	−1.70	–	–	–	–
−40	3.95	3.27	1.89	0.48	−1.39	−2.89	–	–	–	–
−20	2.74	4.60	3.06	0.80	−1.15	−2.63	–	–	–	–
0	3.64	2.11	4.07	−0.53	−0.99	−2.45	–	–	–	–
20	4.59	0.50	2.83	−0.07	−1.78	−2.42	–	–	–	–
40	−2.41	0.72	1.98	0.06	−1.51	−0.80	–	–	–	–
60	−1.97	0.80	1.84	0.33	0.27	−0.80	2.62	2.73	0.05	−2.25
80	–	–	–	–	−0.25	−1.28	2.78	2.34	1.03	−2.10
100	–	–	–	–	0.79	−1.73	3.44	2.43	1.37	−2.10
120	–	–	–	–	0.33	−1.48	1.63	2.68	0.76	−2.35
140	–	–	–	–	−1.29	−2.94	−0.69	0.33	1.09	−2.75
160	–	–	–	–	–	−5.68	−3.16	−0.41	−1.54	−4.80

Table 9. Comparison of computed and actual I_{sc}, 10 Ω-cm cells (% difference)

Temperature, °C	Solar intensity, mW/cm²									
	5.00	25.00	50.00	100.00	140.00	250.00	400.00	550.00	700.00	850.00
−160	−16.27	–	–	–	–	–	–	–	–	–
−140	−5.41	−1.26	–	–	–	–	–	–	–	–
−120	−3.26	1.44	0.94	–	–	–	–	–	–	–
−100	−3.73	1.17	0.59	0.10	–	–	–	–	–	–
−80	−4.05	0.52	0.02	−1.09	−1.43	–	–	–	–	–
−60	−4.45	−0.98	0.63	−2.80	−1.69	−1.91	–	–	–	–
−40	0.50	−0.55	0.44	−1.92	−1.70	−1.34	–	–	–	–
−20	3.20	0.25	0.70	−1.17	−0.48	−0.55	–	–	–	–
0	4.46	1.43	3.03	0.03	−0.16	−0.61	–	–	–	–
20	7.47	2.15	2.33	0.58	−0.71	−0.17	–	–	–	–
40	7.21	2.46	2.11	1.02	1.21	0.34	–	–	–	–
60	6.11	2.10	1.31	0.54	0.82	−0.12	2.58	1.20	3.21	5.69
80	–	–	–	–	−0.36	−1.50	1.62	0.53	3.02	6.53
100	–	–	–	–	−2.11	−1.16	0.72	0.05	3.53	8.21
120	–	–	–	–	−4.91	−1.77	0.95	1.60	6.75	13.34
140	–	–	–	–	−2.39	−1.77	5.02	9.90	16.33	23.78
160	–	–	–	–	–	13.26	19.39	26.32	34.67	43.01

Parametric data uncertainty is propagated through the prediction calculation by means of a series of repeated predictions, as described in the preceding paragraph. However, between predictions, each parametric data point is modified by adding to it the product of its standard deviation and a restricted random number function R, with an average value of zero and a standard deviation of one. After an appropriate number of iterations, the average and standard deviation of the various predictions are taken.

This method is the most accurate of the three; however, it is also the most inconvenient to use as the entire array of parametric data characterizes a particular cell type.

V. Conclusions

The following conclusions are based on the results of the experimental solar test program and the solar cell prediction models discussed in this report:

(1) The 2 Ω-cm cells are suitable for standard cells up to intensities of at least 850 mW/cm² (at a reference temperature of 28°C); 10 Ω-cm cells are suitable up to 250 mW/cm². Beyond that, the I_{sc} of the 10 Ω-cm cells falls off from a linear function of intensity.

(2) For near-Sun missions, 2 Ω-cm cells should be selected for use over 10 Ω-cm cells, since above 250 mW/cm² the P_{mp} of the latter falls off with respect to the P_{mp} of the former.

(3) Deviation in P_{mp} at the high- and low-intensity extremes (as reflected by standard deviations) indicates that for inner and outer planet missions further attention must be focused on cell fabrication processes, proper selection of materials, and cell screening techniques in order to ensure optimum solar array performance.

(4) Analytical expressions derived from parametric data (method 2) and a computer program interpolation scheme (method 3) can be used to accurately reproduce the laboratory solar cell parametric data over a wide range of temperature and intensity.

References

1. Patterson, R. E., Yasui, R. K., and Anspaugh, B., "The Determination and Treatment of Temperature Coefficients of Silicon Solar Cells for Interplanetary Spacecraft Application," Records of the 7th Intersociety Energy Conversion Engineering Conference, San Diego, Calif., Sept. 25–29.
2. Yasui, R. K., and Schmidt, L. W., "Performance Characteristics of Titanium–Silver Contracted N/P and P/N Silicon Solar Cells," Records of the 8th Photovoltaic Specialists Conference, IEEE, Seattle, Wash., Aug. 1970, pp. 110–122.
3. Dash, W. C., and Newman, R., "Intrinsic Optical Absorption in Single Crystal Ge and Si at 77°K and 300°K," *Phys. Rev.*, Vol. 99, 1955, p. 1151.
4. Sandstrom, J. D., "A Method For Predicting Solar Cell Current–Voltage Curve Characteristics as A Function of Incident Solar Intensity and Cell Temperature," Records of the 6th Photovoltaic Specialists Conference, IEEE, Cocoa Beach, Fla., March 28–31, 1967.